Shi, Xuetong; Yazdani, Maryam R.; Ajdary, Rubina; Rojas, Orlando J.

Leakage-proof microencapsulation of phase change materials by emulsification with acetylated cellulose nanofibrils

Published in:
Carbohydrate Polymers

DOI:
10.1016/j.carbpol.2020.117279

Published: 15/02/2021

Document Version
Peer-reviewed accepted author manuscript, also known as Final accepted manuscript or Post-print

Please cite the original version:
Shi, X., Yazdani, M. R., Ajdary, R., & Rojas, O. J. (2021). Leakage-proof microencapsulation of phase change materials by emulsification with acetylated cellulose nanofibrils. *Carbohydrate Polymers*, *254*, Article 117279. https://doi.org/10.1016/j.carbpol.2020.117279

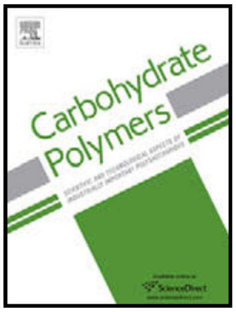

Leakage-proof microencapsulation of phase change materials by emulsification with acetylated cellulose nanofibrils

Xuetong Shi (Conceptualization) (Formal analysis) (Writing - original draft), Maryam R. Yazdani (Conceptualization) (Supervision) (Writing - review and editing), Rubina Ajdary (Conceptualization) (Supervision) (Writing - review and editing), Orlando J. Rojas (Conceptualization) (Supervision) (Resources) (Writing - review and editing)<ce:contributor-role>Funding aquisition)

PII: S0144-8617(20)31452-1

DOI: https://doi.org/10.1016/j.carbpol.2020.117279

Reference: CARP 117279

To appear in: *Carbohydrate Polymers*

Received Date: 10 August 2020

Revised Date: 13 October 2020

Accepted Date: 16 October 2020

Please cite this article as: Shi X, Yazdani MR, Ajdary R, Rojas OJ, Leakage-proof microencapsulation of phase change materials by emulsification with acetylated cellulose nanofibrils, *Carbohydrate Polymers* (2020), doi: https://doi.org/10.1016/j.carbpol.2020.117279

Leakage-proof microencapsulation of phase change materials by emulsification with acetylated cellulose nanofibrils

Xuetong Shi[a], *Maryam R. Yazdani*[b,*], *Rubina Ajdary*[a], *Orlando J. Rojas*[a,c,*]

[a] Department of Bioproducts and Biosystems, Aalto University, Espoo 02150, Finland

[b] Department of Mechanical Engineering, Aalto University, Espoo 02150, Finland

[c] Bioproducts Institute, Departments of Chemical & Biological Engineering, Chemistry, and Wood Science, 2360 East Mall, The University of British Columbia, Vancouver, BC V6T 1Z3, Canada

Graphical abstract

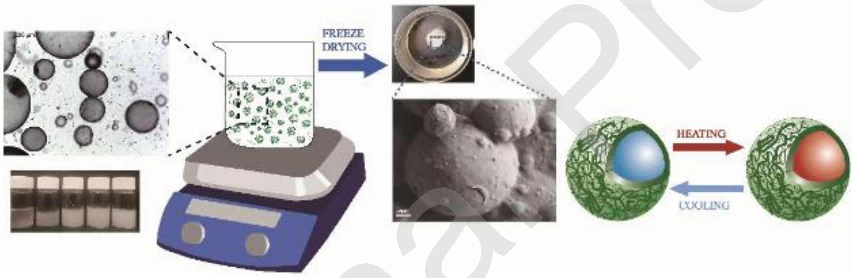

Acetylated cellulose nanofibrils are usedto encapsulate paraffin, forming shape-stable phase changesystemssuitable for thermal energy storage and conversion.

Highlights

- Acetylated nanocellulose enables shape and thermally-stable paraffin encapsulation.
- The leakage-free phase change material withstands cyclic melting/solidification.
- A high melting enthalpy (173 J/g) and reduced supercooling (by 53%) are observed.
- The results indicate stable and durable solution for energy conversion/storage.

ABSTRACT

We use acetylated cellulose nanofibrils (AcCNF) to stabilize transient emulsions with paraffin that becomes shape-stable and encapsulated phase change material (PCM) upon cooling. Rheology measurements confirm the gel behavior and colloidal stability of the solid suspensions. We study the effect of nanofiber content on PCM leakage upon melting and compare the results to those from unmodified CNF. The nanostructured cellulose promotes paraffin phase transition, which improves the efficiency of thermal energy exchange. The leakage-proof microcapsules display high energy absorption capacity (ΔH_m=173 J/g) at high PCM loading (up to 80 wt%), while effectively controlling the extent of supercooling. An excellent thermal stability is observed during at least 100 heating/cooling cycles. Degradation takes place at 291 °C, indicating good thermal stability. The high energy density and the effective shape and thermal stabilization of the AcCNF-encapsulated paraffin points to a sustainable solution for thermal energy storage and conversion.

Keywords: Phase change material, PCM, paraffin, acetylated cellulose nanofibril, encapsulation, heat storage.

1. Introduction

The worldwide increase in energy consumption has become increasingly important given the imminent effects of climate change and air pollution (Perera, 2018). Thus, there is a significant need to develop renewable and sustainable energy solutions. In this context, phase change materials (PCM) are of great interest since they display a high latent heat that can be exchanged or stored during physical phase transitions, within an appropriate temperature range (Fleischer, 2015; Veerakumar & Sreekumar, 2016). With such abilities, PCMs have been proposed for energy storage and temperature regulation in buildings (Kośny, 2015; Telkes, 1980; Veerakumar & Sreekumar, 2016), solar water heating (Mahfuz, Anisur, Kibria, Saidur,

& Metselaar, 2014) and thermo-regulating textiles (Mondal, 2008; Sarier & Onder, 2012).

Paraffin, a common organic PCM, provides the advantages of high latent heat, chemical stability, non-corrosiveness, relative affordability while showing no phase segregation during phase transition (Gulfam, Zhang, & Meng, 2019; Safari, Saidur, Sulaiman, Xu, & Dong, 2017). Unfortunately, the effects of leakage and supercooling challenges the use of paraffin in the melt state. The latter phenomenon, supercooling, occurs when PCM crystallizes at a temperature below its theoretical freezing point, implying a higher energy demand for the PCM to undergo phase transition. This reduces the PCM´s working efficiency, directly associated with heat exchange. The supercooling effect can be minimized by addition of nucleation agents that can accelerate crystallization (Safari et al., 2017). On the other hand, leakage can be avoided or minimized by protecting or containing the PCM by encapsulation (Huo et al., 2018; Shchukina, Graham, Zheng, & Shchukin, 2018) or entrapping it in porous structures (Atinafu et al., 2018; Sheng, Nomura, Zhu, Habazaki, & Akiyama, 2019; Xiao & Zhang, 2013). Such strategies involve either physically adsorption (Sheng et al., 2019; Xiao & Zhang, 2013; Zhao et al., 2019), chemically bonding (Hassabo & Mohamed, 2017; Qian et al., 2019) or ionic cross-linking (Yazdani et al., 2020) between the PCM and the supporting materials.

Organic polymers have been studied as rigid and leakage-proof shell structures for organic PCMs. They include poly(urea-urethane) (Yoo, Martinez, & Youngblood, 2017), polystyrene copolymers (W. Li et al., 2011; Maleki et al., 2019) and polyethylene terephthalate (Chen, Wang, & Huang, 2008). Other organic materials, for instance, graphene oxide (Zhao et al., 2019) and multi-walled carbon nanotubes (Tang, Sun, Yu, & Wang, 2014), have been reported as suitable supports of paraffin. However, considering the increasing environmental pressures, there is a demand for biobased alternatives for encapsulation, e.g., to substitute synthetic materials. Nanocelluloses, including cellulose nanofibrils (CNF), derived from natural resources, such as plants and microorganisms, offer an opportunity given that they are compatible with both oil and water phases, are capable of encapsulating oil droplets and keep the system colloidally stable (Kalashnikova, Bizot, Cathala, & Capron, 2011; Y. Li et al., 2017; Mikulcová, Bordes, & Kašpárková, 2016; Svagan et al., 2014). Given its abundant hydroxyl groups, unmodified CNF forms a hydrogel in water. However, due to the hydrophobic nature of paraffin PCM, appropriate CNF chemical modifications may be needed, for example to lower its surface energy and to enhance its compatibility with paraffin, the encapsulation process and the thermal durability of the resulting system. For instance, acetylation reduces cellulose hydrophilicity (Tripathi, Ago, Khan, & Rojas, 2018; Beaumont et al., 2020) owing to the partial replacement of hydroxyl groups and reduction of inter- and intra-hydrogen bonding. As such, an improved compatibility between the PCM and acetylated CNF, herein referred to as AcCNF, is hypothesized to enhance encapsulation and energy storage efficiency. A higher mechanical strength can be achieved through the heterogeneous acetylation, as has been ascribed to the retention of the fibril morphology and structure, without compromising the degree of substitution (Tripathi, Ago, Khan, & Rojas, 2018). The introduction of acetylated group can also enhance the thermal stability of native cellulose (Nogi et al., 2006; Yang et al., 2018) while reducing moisture sorption. Given its size, nanocellulose has a great potential for incorporation in PCMs. In addition, it can act as nucleating agent for crystallization and to accelerate PCM´s solidification, to reduce the degree of supercooling. Therefore, we hypothesize that acetylated nanocellulose offers potential as supporting and encapsulation medium for PCMs. In this work, we used AcCNF to encapsulate paraffin and to form shape-stable phase changing systems (**Figure S1**). We demonstrate the compatibility of paraffin with AcCNF makes the latter an ideal supporting material for thermal energy storage.

2. Experimental

2.1 Materials. Paraffin (melting point 52-54 °C, 0.9 g/cm³ at 20 °C) was purchased from VWR Chemicals. Cellulose nanofibrils (CNF) were produced from fines-free bleached sulfite birch fibers sourced from a Finish pulp mill. The latter were subjected to microfluidization, as described by Guo et al. (Guo, Filpponen, Su, Laine, & Rojas, 2016). The dry matter content of the obtained CNF suspension was 1.77 wt%. Acetylated cellulose nanofibrils (AcCNF) were produced by heterogeneous acetylation on the Kraft birch wood to achieve acetylated cellulosic fibers which were also microfluidized to produce acetylated CNF, AcCNF (Tripathi et al., 2018). The acetylation procedure comprised three solvent exchanges at first followed by chemical reaction with acetic anhydride under constant stirring at room temperature. The acetylated cellulose fibers were microfluidized using one pass at a 1500 bar through chambers of 400-200 micrometer. The obtained AcCNF had a dry matter content of 0.54 wt% (± 0.05) and a degree of substitution of 0.6.(Tripathi et al., 2018)

2.2 PCM-nanocellulose suspension. A given mass of paraffin was mixed with AcCNF suspension (or CNF, used as a reference) using a magnetic stirrer (500 rpm) at 80 °C for 20 min, achieving an emulgel. The resultant PCM/water emulsions were prepared in replicates and stabilized by the respective nanocellulose using given paraffin-to-nanofibrils ratios, namely, 60/40, 70/30, 80/20, 90/10 (wt%, dry basis). The dispersed phase in the emulsion solidified upon cooling, producing solid particle suspensions and particle morphology and rheology were assessed. Some of the samples were freeze-dried for further analyzes (morphology, thermal and stability tests). **Table 1** includes the nomenclature and composition of the samples.

2.3. Suspension Morphology. The samples were observed under a light microscope (Leica MD750, Switzerland) and capsule size distribution was determined in the suspension. One hot droplet of the fresh suspension sample was placed on the glass micro-slide and a covered with a coverslip. The thin layer samples were then observed under 10, 20, and 40x magnification.

Table 1. Composition of emulsions prepared by magnetic stirring using nanofibrils (CNF or AcCNF) as stabilizers and further used as precursors for paraffin microcapsules suspended in

water.

Name	**Support**	**Paraffin (wt%)**	**Nanofibrils (wt%)**
A1	AcCNF	60	40
A2	AcCNF	70	30
A3	AcCNF	80	20
A4	AcCNF	90	10
A5	AcCNF	91	9
A6	AcCNF	92	8
C1	CNF	60	40
C2	CNF	70	30
C3	CNF	80	20
C4	CNF	90	10

2.4. Rheology. The rheological behavior of the suspensions was studied by using shear and frequency sweep profiles that were acquired with a dynamic rotational rheometer (MCR 302, Anton Paar, Germany). A parallel plate geometry (PP25) with smooth surfaces was used at shear rate between 0.01 and 100 s^{-1}. The gap between the parallel plates was set at 1 mm. Frequency sweep measurements were conducted at an angular frequency of 0.1-100 rad/s. The stress sweep tests were carried out at an angular frequency of 10 rad/s. A constant strain of 0.5% was applied in all rheological measurements, in the linear viscoelastic region. The rheology tests were conducted with 0.5 wt% acetylated nanocellulose and samples A1-A6, C1-C4 (**Table 1**). The temperature was kept at 23 °C.

2.5. Morphology of encapsulated PCM. The morphology of the solid suspended PCM particles was studied under scanning electron microscopy (SEM) using a Zeiss Sigma VP scanning electron microscope (Germany). The freeze-dried samples were prepared and fixed on the metal sample stub using a carbon double-sided tape and then were sputter-coated with a 4 nm thickness Platinum-Palladium coating (LECIA EM ACE600 sputter coater). The SEM images were taken under vacuum condition at 2 kV.

2.6. Phase change properties. The thermal properties of the samples were examined using differential scanning calorimetry (NETZSCH DSC 204F1 Phoenix, Germany). Typically, a 5-10 mg amount of sample was placed in aluminum crucibles and heated from 0 °C to 70 °C (5 K/min rate) in a nitrogen atmosphere. The DSC program included four heating and cooling cycles at 5 K/min scan rate. The data from the third cycle were collected to record the latent heat, specific heat, melting temperature (T_m), and crystallization temperature (T_c), the mean value and the standard deviation of the replicates are reported. To study the thermal stability and repeatability, the DSC measurements were conducted under 100 consecutive heating and cooling cycles, using the same conditions as reported above.

2.7. Thermal stability. The thermal stability and the compositional degradation of the encapsulated PCM were studied using thermogravimetric analysis on a NETZSCH STA 449F3 instrument (TYPE: ANSI, Germany). The samples were heated from 40 °C to 500 °C in helium gas atmosphere, at a 5 K/min heating rate.

2.8. Chemical compatibility and stability. FTIR-ATR measurements were conducted to confirm any reaction between cellulose and paraffin (PerkinElmer spectrometer, Spectrum Two Polymer QA/QC Analysis System, USA) using a diamond crystal. The spectra were firstly scanned using background removal, and when the baseline was corrected at wavenumber set at 400-4500 cm-1 for transmittance. The X-ray diffraction (XRD) patterns of the samples were measured using an X-ray diffractometer (Rigaku SmartLab X-Ray Diffractometer) equipped with Cu-Ka radiation, in the 2θ range of 5º–60º with a step interval of 0.02º.

3. Results and discussion

3.1 AcCNF-PCM colloidal suspension, microstructure and stability. The preparation of AcCNF-paraffin emulsions was performed at 80 ºC, with paraffin in the liquid state. The paraffin droplets were stabilized and later encapsulated by nanocellulose soon after cooling to room temperature. **Figure 1a,1b** and **S2a-d** show the presence of paraffin spheres (diameter of

50-300 μm) surrounded by cellulose nanofibrils, which acted as stabilizing agent. AcCNF formed a network structure around the paraffin droplets, resulting in stabilization while undergoing from the melt phase (emulsion, liquid droplets) to solid spheres. In the aqueous system, acetylated cellulose fibrils adsorbed at the oil-water interface by secondary interactions.

The rheology tests were conducted with AcCNF-paraffin colloidal suspensions to study the gelling behavior and stability of the precursor material. The prepared AcCNF-paraffin colloidal suspensions were gel-like (**Figure 1c**). The precursor suspensions of different compositions were shear thinning, similar to the aqueous AcCNF suspension (**Figure 1d**). This suggests that the addition of paraffin does not break down the original AcCNF network structure. The latter and the colloidal properties of AcCNF suspensions are preserved after the process of encapsulation; both, the AcCNF and paraffin/AcCNF capsule suspensions show gel stability (see results from oscillatory frequency and stress sweep, **Figure S2e,f**).

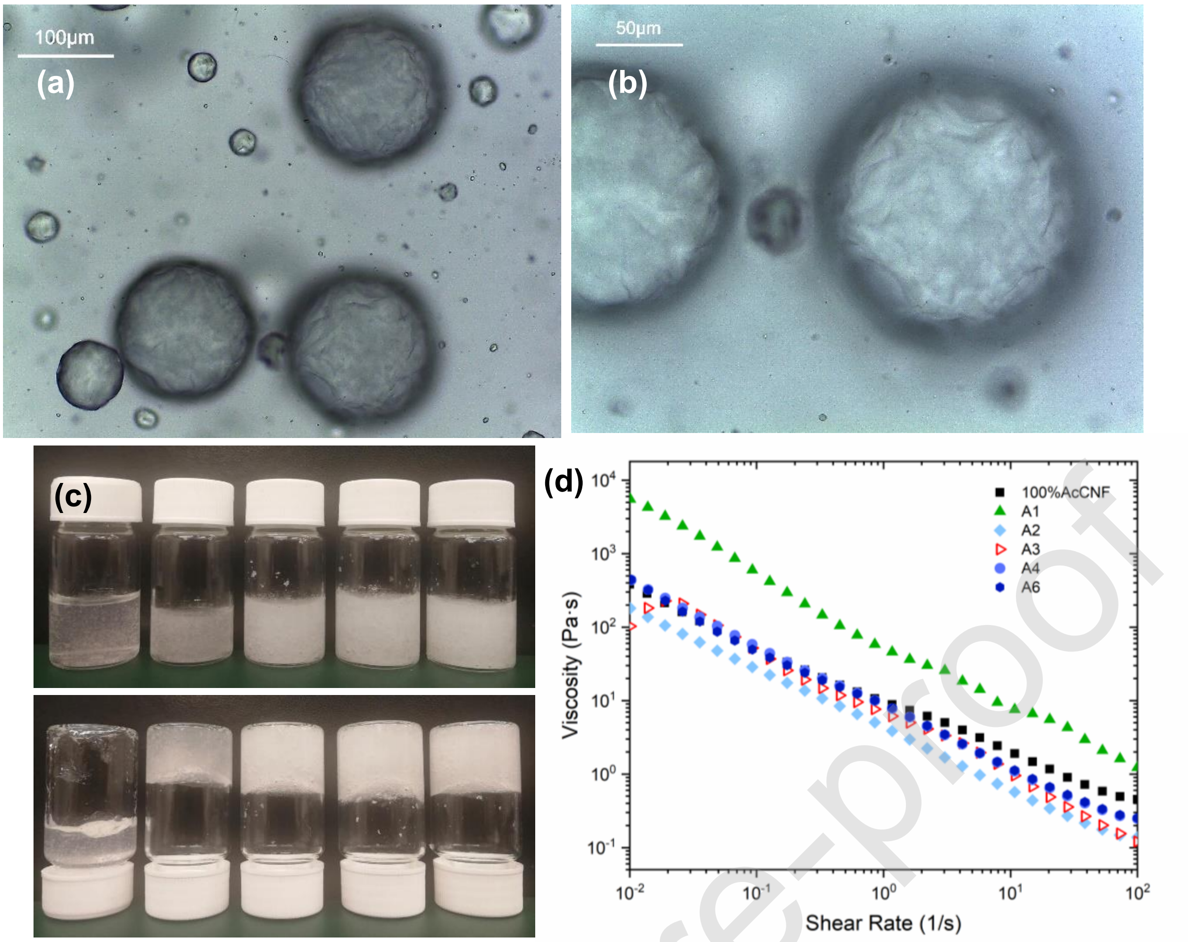

Figure 1. (a and b) Light microscopy images showing the microstructure of the colloidal suspension (paraffin capsules) at different magnifications. (c) AcCNF-PCM colloidal suspensions corresponding to samples (from left to right): A2, A3, A4, A5, A6. (d) Shear thinning behavior of AcCNF and AcCNF-PCM (A1, A2, A3, A4 and A6) colloidal suspensions.

3.2 Morphology of encapsulated paraffin. Solid capsules comprising paraffin were produced upon freeze drying of the AcCNF-paraffin colloidal suspension. Nanocellulose formed a robust microcapsule shell structure (SEM in **Figure 2**). Paraffin shows as a flake-like material, as shown in **Figure 2a**. With the incorporation of AcCNF, paraffin microcapsules are stabilized. The original crystal structure and organization of paraffin changed since the alkane chains do not stack together upon AcCNF addition, e.g., the crystallinity of paraffin is reduced (**Figure S5**). The fibrils and fibril bundles are adsorbed and are observed on the surface of the microcapsules, **Figure 2b.** Unmodified CNF was used to encapsulate paraffin (**Figure S2h**); however, given the higher hydrophilicity, a lower compatibility with paraffin was noted, limiting the robustness of the system.

Figure 2c and 2d, show fibrils at different scales adsorbed on the paraffin/AcCNF interface, taking part in the formation of a shell structure. Cellulose microfibrils (shown with the yellow circle) and nanofibrils (shown inside the red circle) in the AcCNF suspension both contribute to the shell structure formation and the stabilization of the paraffin microcapsules (Tripathi et al., 2018). The shell formed by fibrils of different sizes preserve the paraffin from leaking when the temperature is raised above the melting point. The adsorption of AcCNF to paraffin and the microcapsule structure formation rely on surface tension, capillary force and secondary interactions (Qi, 2017; Wadsö, 1995). This lack of chemical interactions is confirmed by FTIR (**Figure S3 and S4**) and XRD (**Figure S5**), which showed no new peaks in the AcCNF-encapsulated paraffin. Physical adsorption and the oil interactions via AcCNF hydrophobic groups contributes to a porous microstructure. Molecular dynamics (MD) simulation indicates that both enthalpic and entropic effects drive the adsorption process (Y. Li et al., 2017).

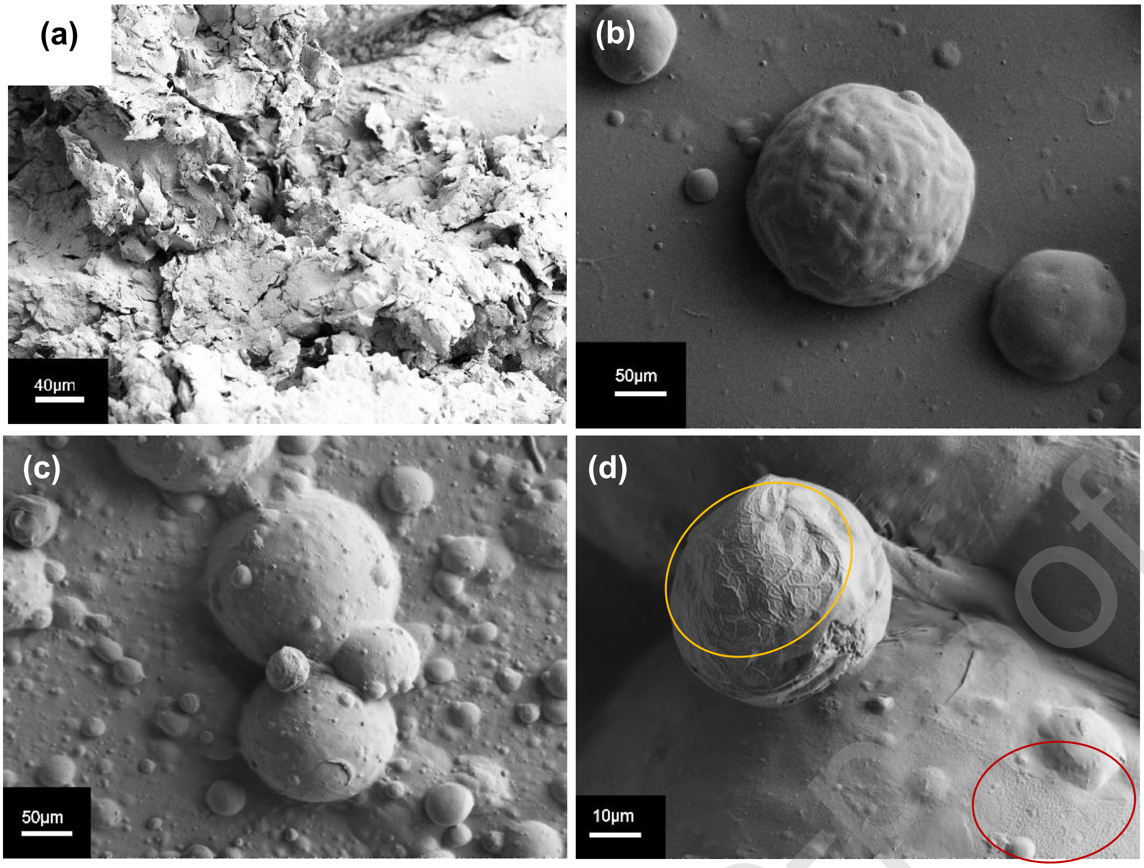

Figure 2. SEM images of (a) pure paraffin (PCM) and paraffin microcapsules: (b) A2, (c, d) A5.

3.3 Thermal energy storage. The thermal energy storage of the encapsulated paraffin, as measured by the phase change temperature, enthalpy and thermal cycling behavior was studied by DSC. When comparing the melting and solidification enthalpies of the given samples, it becomes apparent that the paraffin encapsulated by AcCNF gives a higher latent heat as well as a better encapsulation ratio (R) than that provided by unmodified CNF, **Figure 3 and Table 2**. This may be due to partial replacement of hydroxyls in CNF by acetyl groups, making AcCNF less hydrophilic and more compatible with the non-polar paraffin. The improved hydrophobicity of acetylated fibrils also makes them to maintain a larger surface area upon water removal (Kim et al., 2002), providing better compatibility with the hydrophobic phase, namely, incorporating more paraffin in the capsules and resulting in a higher latent heat. The better colloidal stability and compatibility of paraffin with AcCNF improves the interfacial interaction between the two components (Taib, Yehye, Julkapli, & Hamid, 2018). In contrast, the interactions with paraffin are limited in the case of unmodified CNF. This is because of the CNF strong inter and intra-hydrogen bonding, the higher surface energy and interfacial area (**Figure S2 h**). In sum, AcCNF facilitates the formation of paraffin capsules and the storage of latent heat. The latent heat adsorbed and released increases by increasing the paraffin content, an effect that is observed for both type of nanofibrils (see **Figure 3a-d** for the thermal properties of samples A1, A2, A3 and A4). The raise in paraffin latent heat is shown from the enthalpy change (DSC measurements, **Figure 3e**). The sample with 80 % paraffin (A3) provides up to 173 J/g latent heat of fusion while that with 20 % AcCNF content prevents the leakage of molten paraffin (see Section 3.4, **Figure 6**). Previously, a form-stable paraffin was prepared with silica and expanded graphite (EG), which exhibited a latent heat of 104 J/g (M. Li, Wu, & Tan, 2012). Likewise, an epoxy resin sealed expanded graphite/paraffin composite PCM exhibited a latent heat of 137 J/g with 94% paraffin (Ren, Shen, Yang, & Yang, 2019). Graphite oxide was also utilized to encapsulate paraffin by using Pickering emulsions, achieving only a limited efficiency, < 10% (Zhao et al., 2019). In the context of biobased supporting materials, AcCNF-supported PCM exhibits high encapsulation efficiency and good thermal energy storage properties. For example, chitosan produced an paraffin encapsulation efficiency of 49.8% (Huo et al., 2018), while 62% encapsulation ratio was obtained for ethyl cellulose (Lin et al., 2018) and a 42 % efficiency was reported for polylactic acid (Fashandi et al., 2017).

By the incorporation of either acetylated CNF or unmodified CNF, the phase change properties showed similar tendency: the melting temperature (T_m) moves to a lower value while the freezing point (T_c) shifts to higher degrees (**Figure 3f**). A lower melting point, indicated by the incorporation of nano-sized cellulose, helps to improve the melting process (Al-Jethelah, Tasnim, Mahmud, & Dutta, 2018). In these conditions, paraffin solidification accelerates since nanocellulose works as a nucleating agent, presenting sites for a faster crystallization of paraffin. Taken together, the results indicate a reduced supercooling (as measured by the differences between the Tm and Tc (ΔT), **Figure 3f** and **Table 2**). This effect suggests that a lower activation energy is needed for phase transition (Debenedetti & Stillinger, 2001). Large supercooling causes a larger activation energy for solicitation at the fusion temperature of the PCM, so that the PCM remains in the liquid state at a point when it is supposed to crystallize. This delays the release of the stored energy (Safari et al., 2017) and reduces energy utilization efficiency. Thus, prevention of supercooling helps to convert thermal energy more effectively. Cellulose nanofibrils function as a nucleating agent for solidification, which accelerates the crystallization of PCM (Du, Wu, Yan, Kortschot, & Farnood, 2014; Khoo, Ismail, & Chow, 2016; J. Li, Lu, Zeng, & Luo, 2014). As a result, the stored heat energy can be released sooner and more effectively. As seen in **Figure 3f**, unmodified CNF works more effectively as far as the supercooling effect. By increasing the fibrils content from 10 wt% to 40 wt%, the supercooling extent is reduced by CNF, from 17.8 °C to the lowest value, 7.2 °C (about 60% reduction efficiency). Meanwhile, the respective value for the AcCNF-stabilized system is 8.4 °C (53% efficiency) (**Figure 3, Table 2**). The higher efficiency of unmodified CNF in reducing supercooling is likely the results of the lower interactions between paraffin and the supporting network (a lower activation energy to overcome the start of crystallization is needed if CNF is used).

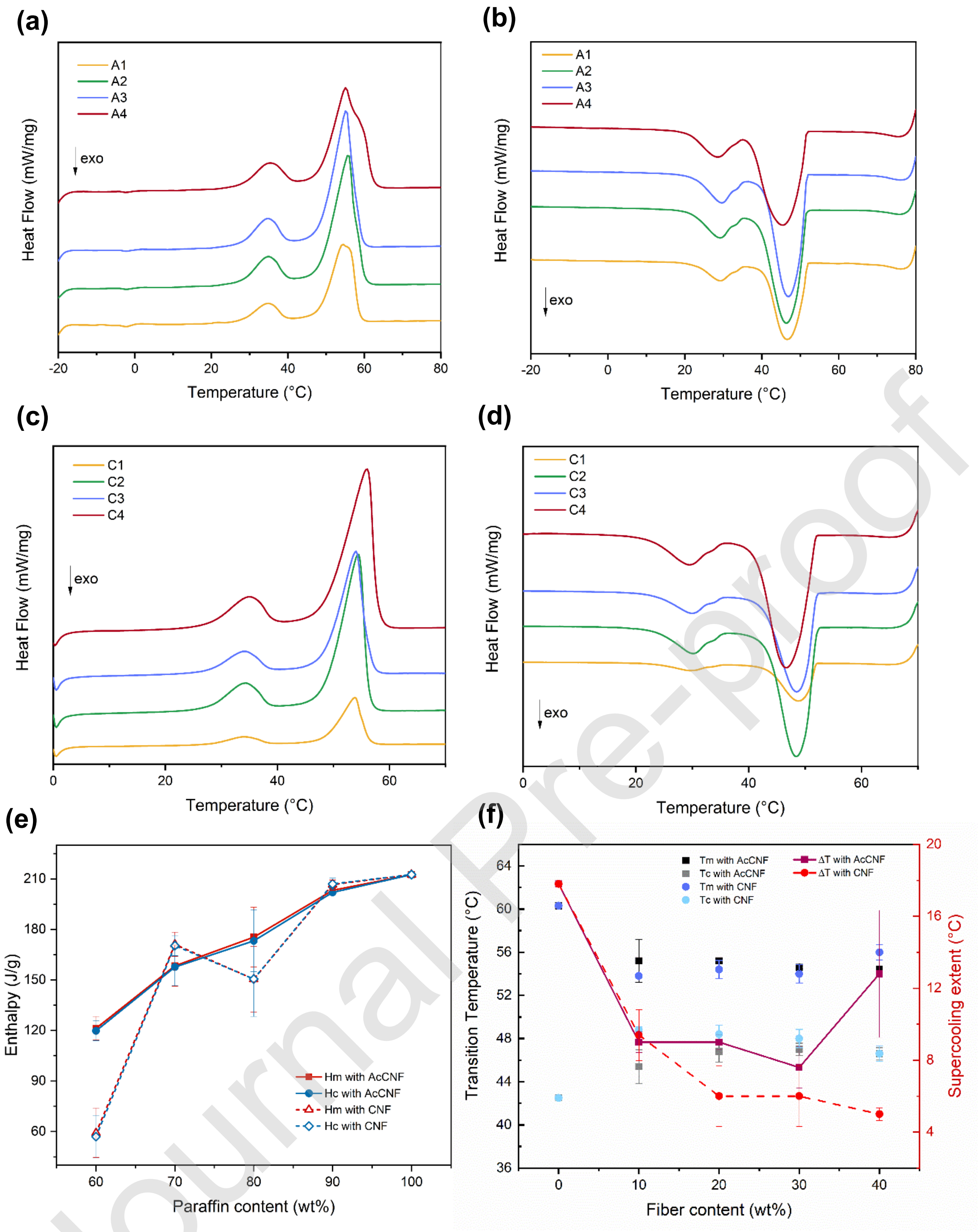

Figure 3. DSC data upon heating (a, c) of paraffin encapsulated by AcCNF and unmodified CNF. Also, data is shown for the cooling procedure (b, d) paraffin encapsulated by AcCNF and CNF. (e, f) Phase change enthalpy and transition temperature of encapsulated paraffin.

Table 2. Latent heat of melting (ΔH_m), latent heat of solidification (ΔH_c), melting temperature (T_m), crystallization temperature (T_c) and supercooling extent (ΔT) for the respective samples

is listed along R, the effective enthalpy ratio. ΔH_m and ΔH_c were measured from the area under the phase transition peaks in the DSC profiles. T_m is the melting temperature from the DSC data. Likewise, T_c is the crystallization temperature of phase transition and ΔT is the temperature difference between T_m and T_c. The DSC measurements were obtained using samples that were run in four replicates and the average value and the standard deviation are reported.

Samples	**ΔH_m (J/g)**	**ΔH_c (J/g)**	**T_m (°C)**	**T_c (°C)**	**ΔT (°C)**	**R (%)$^{(*)}$**
Paraffin	212.5	212.5	60.3	42.5	17.8	100
A1	121.4±0.1	119.8±0.1	55.8±2.0	45.5±1.6	10.3±3.5	56.8
C1	59.2±14.7	57±12.6	53.8±0.1	49.0±0.3	4.75±0.4	27.7
A2	171.0±17.8	170.6±18.2	54.7±0.1	46.3±1.0	8.4±1.1	80.5
C2	171.1±7.1	170.4±6.0	55.0±0.8	47.8±0.8	7.2±1.7	80.2
A3	184.0±12.1	181.0±11.0	55.1±0.1	46.4±0.6	8.7±0.4	86.1
C3	150.5±19.5	150.6±22.3	54.6±0.8	47.4±0.8	7.2±1.7	70.9
A4	198.3±7.0	197.9±5.9	55.2±0	45.8±0.6	9.4±0.6	93.0
C4	206.6±2.7	207±3.4	55.5±0.7	47.1±0.7	8.4±1.4	97.4

$^{(*)}$ *Note: R is the effective enthalpy ratio of the encapsulated paraffin, calculated from:* $R = \frac{\Delta H_{c,encap.}}{\Delta H_{c,PCM.}} \times 100\%$ *(Atinafu et al., 2018 & Meng et al., 2020) with* $\Delta H_{c,encap.}$ *and* $\Delta H_{c,PCM}$ *the crystallization enthalpy of the encapsulated paraffin and paraffin, respectively.*

The specific heat capacity of AcCNF and encapsulated paraffin (for different compositions and at different temperatures) are included in **Figure 4**. The lowest specific heat capacity appears at T< 10 ºC, for AcCNF, paraffin and encapsulated PCM, when they are in the solid state. Their highest C_p occurs at ~58ºC when melting occurs, for both paraffin and the prepared samples. The C_p of AcCNF is fairly constant as the temperature increases. A similar tendency is observed for all materials, i.e., the melt material (T=70ºC) has a higher C_p than the solid counterpart (T=10ºC) (**Table 3**). The specific heat capacity of encapsulated paraffin samples at different temperatures is increased with a higher paraffin loading, which indicates an increased heat absorption and release ability. The paraffin encapsulated by unmodified CNF shows similar performance (**Figure S6**), the developed materials do not affect the original Cp value of paraffin.

Table 3. The specific heat capacity of samples at their solid and melt state.

Specific Heat Cp (J/g·K)	Paraffin	AcCNF	A1	A2	A3	A4
T=10ºC	2.01	1.57	1.50	1.59	1.82	1.88
T=70ºC	2.34	2.08	1.93	1.98	2.20	2.24

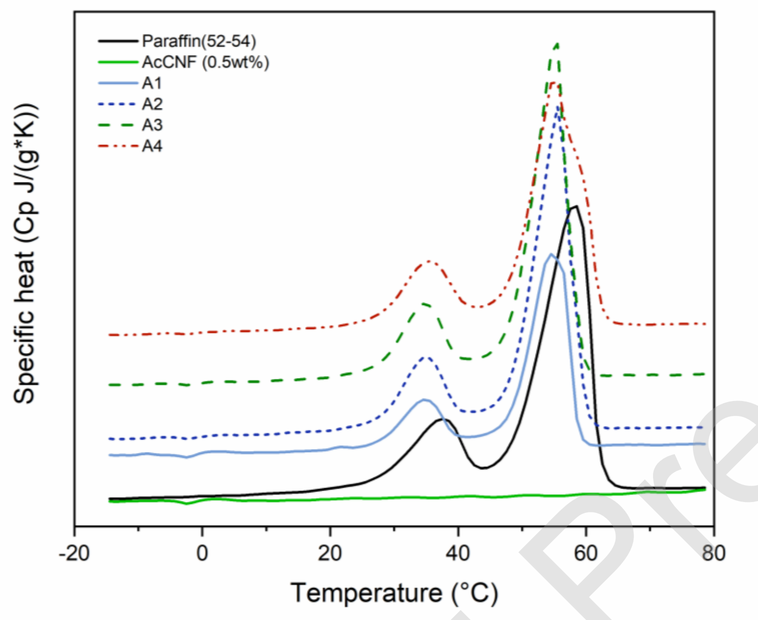

Figure 4. Specific heat capacity of paraffin encapsulated in AcCNF at the given compositions.

3.4 Thermal stability. The thermal stability of the samples was studied by thermogravimetric analysis and the degradation point was obtained with the first order TG differential. As the TG results in **Figure 5a** show, bulk paraffin, AcCNF and encapsulated paraffin have a similar thermal degradation behavior: degradation occurs in a very close temperature region. Within the 0-200 °C temperature region, encapsulated paraffin undergoes no mass loss, suggesting that the paraffin encapsulated in AcCNF is stable in the phase change temperature range (20°C - 70°C). The degradation point is confirmed by the DTG results (the first derivative of the TGA curve), indicating that paraffin totally degrades at 290 °C and AcCNF degrades at 288°C, with approximately 40 wt% residual organic phase. The degradation point is enhanced by the addition of AcCNF: degradation temperature of 298 °C and 291 °C with 30 wt% and 20 wt% AcCNF loading, respectively (samples A2 and A3). TGA results indicate that the thermal stability of paraffin is improved by adding AcCNF, without influencing its original thermal performance and thermal degradation tendency. The high thermal stability of nanocellulose contributes to the better thermal stability of the encapsulated PCM (Mariano, Cercená, & Soldi, 2016; Wei et al., 2019).

The repeatability of phase change properties as well as the shape stability are important criteria in considering PCM systems. Thus, we studied such factors for paraffin encapsulated in AcCNF, after 100 consecutive heating and cooling cycles, **Figure 5b**. As observed, the phase change properties of the encapsulated PCM is highly repeatable, **Figure 5b**. This suggests that the encapsulated paraffin (20 wt% of AcCNF) is a stable system, with reliable thermal properties and presenting excellent durability. The latent heat of melting and cooling recorded in **Table 4** shows almost no visible change in thermal properties after 100 times cycles. Earlier work related to the micro-encapsulation of tetradecane PCM with the aid of zein showed a visible offset of heating and cooling after 100 cycles (Singh, Gaikwad, Lee, & Lee, 2018). A paraffin PCM composite stabilized by cotton-derived sponge indicated a slight shift after 100 cycles, although it demonstrated a very high thermal storage capacity (>200 J/g) (Sheng et al., 2019).

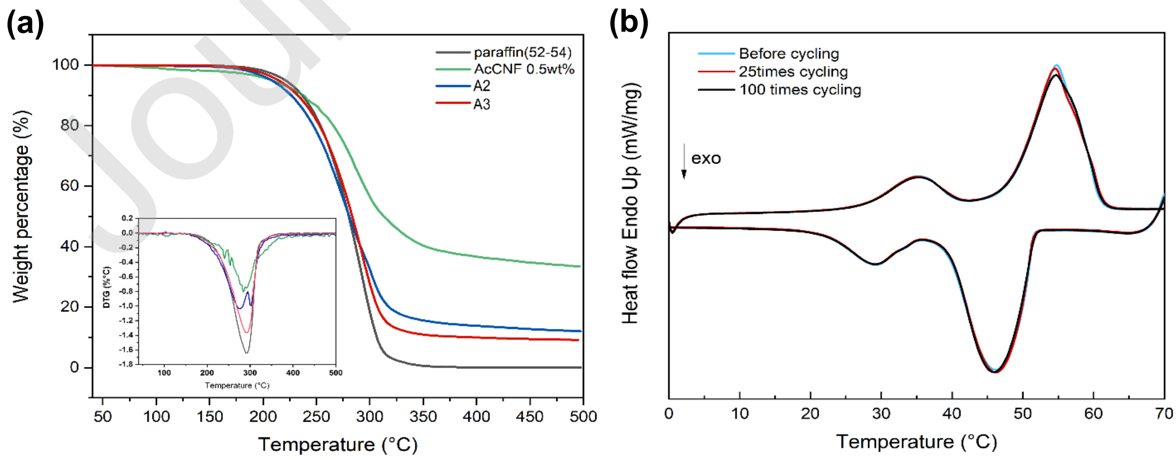

Figure 5. Stability of encapsulated paraffin (a) TG and DTG profiles for paraffin, acetylated nanofibrils (AcCNF) and paraffin encapsulated in AcCNF. (b) Thermal cycling behavior of sample A3 after 50 and 100 consecutive DSC heating/cooling cycles.

Table 4. Thermal properties of the encapsulated paraffin (A3) before and after thermal cycling.

	Tm (°C)	**Tc (°C)**	**ΔHm (J/g)**	**ΔHc (J/g)**
Before cycling	55.0	46.0	172.5	234.0
25 thermal cycles	54.5	46.2	175.6	229.1
100 thermal cycles	54.8	45.8	171.4	231.9

Shape stability and leakage prevention were studied for the encapsulated paraffin with 8, 10, 20 and 30 wt% AcCNF (samples A6, A4, A3, A2), to determine the limit and critical fibril amount leading to leakage-proof systems. Firstly, by checking their appearance to examine if liquid paraffin leaks out, dried encapsulated paraffin samples were heated at 100 °C for 1 h and cooled down to room temperature, **Figure 6a**. The samples with less than 10 wt% fibrils leaked molten paraffin (samples A4 and A6 in **Figure 6a**) while the samples with 20 and 30wt% AcCNF (sample A2 and A3 in **Figure 6a**) were leakage-proof.

The micromorphology of encapsulated paraffin was studied by SEM. After 10 thermal cycles (heating/cooling: heating to 100 ºC for 0.5 h and cooling to room temperature), the morphology of the microcapsule (dried sample A3) was maintained and indicated almost no difference from the original encapsulated PCM (**Figure 6b**). A fine and intact shell layer with fibrils structures can be observed after heating at 100 ºC for 0.5 h, following 10 thermal cycles. The shell layer is smooth, without rupture and no signs of paraffin exist outside the shell, suggesting that the nanofibrils formed a robust capsule that maintained the PCM shape and function. The appearance of a small concave features may be due to the re-solidification of paraffin after melting and the volume change during phase transition.

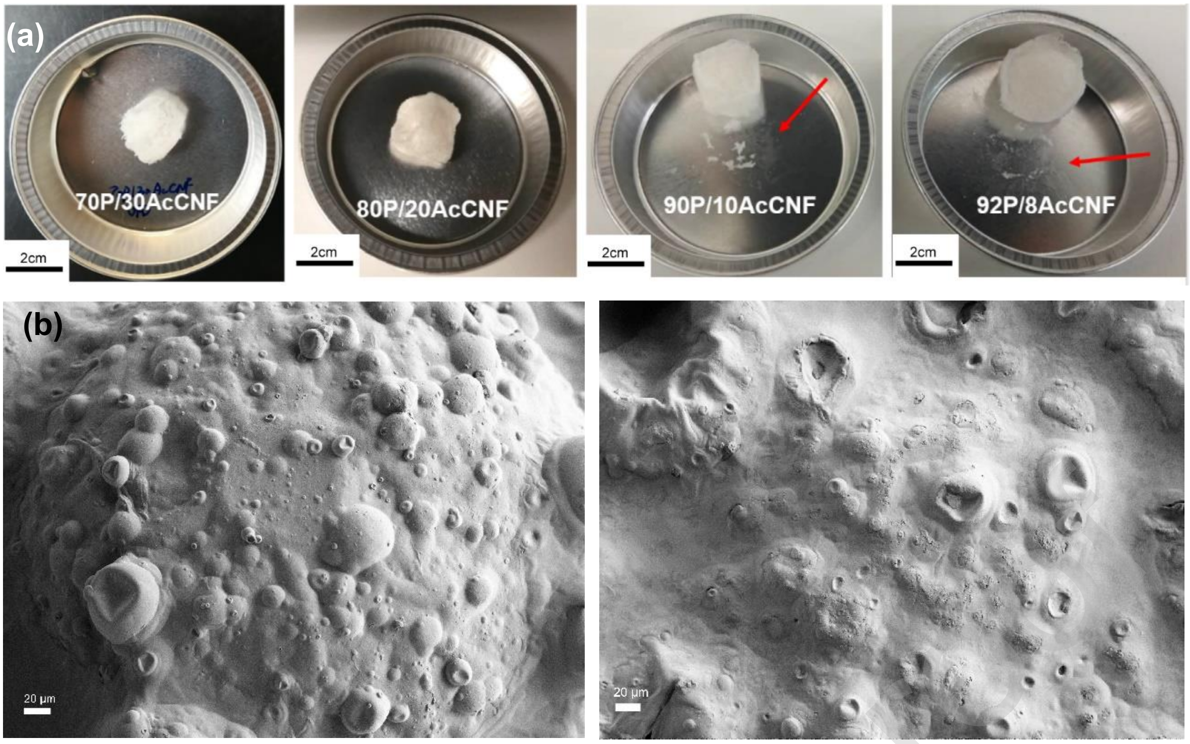

Figure 6. (a) Encapsulated paraffin (samples A2, A3, A4, A6, from left to right) after heating 1h at 100ºC. (b) SEM image of sample A3 before heating (right image) and after 10 cycles heating/cooling (left image).

Conclusions

A leakage-proof PCM is introduced by the incorporation of acetylated nanocellulose in paraffin emulsions that solidified into an aqueous dispersion containing solid microcapsules. The AcCNF network formed on the surface of the capsules works as a supporting matrix that preserve paraffin shape and function and prevents leakage during melting. The as-prepared AcCNF-encapsulated paraffin presents a high melting latent heat (173 J/g) and a reduced supercooling (53% efficiency with 80 wt% paraffin loading). Compared to CNF, the better compatibility of AcCNF with paraffin enhances the encapsulation efficiency and thermal performance. AcCNF acts as nucleation agent that accelerates the heat release process. It also exhibits excellent thermal stability and cyclability after 100 times heating/cooling without phase transition (ΔHm = 171.4 J/g is maintained). The AcCNF-encapsulated paraffin shows a high thermal energy storage density and indicate its potential for thermal energy conversion and solar energy storage, for example, in construction and composite materials.

Credit Author Statement

Xuetong Shi: Conceptualization, Experimentation, Analysis, Writing – Original Draft
Maryam R. Yazdani: Conceptualization, Supervision, Writing – Review & Editing
Rubina Ajdary: Conceptualization, Supervision, Writing – Review & Editing
Orlando J. Rojas: Conceptualization, Supervision, Resources, Writing – Review & Editing, Funding

AUTHOR INFORMATION

Corresponding Authors

*Orlando J. Rojas, Email: orlando.rojas@ubc.ca; Tel: +1-604-822-3457; Maryam R. Yazdani, Email: roza.yazdani@aalto.fi

Author contributions

The manuscript as written through contributions of all authors. All authors have given approval to the final version of the manuscript.

Acknowledgements

We acknowledge Ya Zhu for help in laboratory work and discussions related to material preparation. The authors acknowledge funding from the European Research Council (ERC) under the European Union's Horizon 2020 research and innovation program (ERC Advanced Grant Agreement No. 788489, "BioElCell") and the Canada Excellence Research Chair initiative. M.R.Y. would also like to thank Finnish Cultural Foundation (Suomen Kulttuurirahasto) for financial support.

.

References

Al-Jethelah, M., Tasnim, S. H., Mahmud, S., & Dutta, A. (2018). Nano-PCM filled energy storage system for solar-thermal applications. *Renewable energy,* 126, 137-155.

Atinafu, D. G., Dong, W., Wang, J., Huang, X., Wang, J., Gao, H., & Wang, G. (2018). Synthesis and Characterization of Paraffin/Metal Organic Gel Derived Porous Carbon/Boron Nitride Composite Phase Change Materials for Thermal Energy Storage. *European Journal of Inorganic Chemistry,* 2018(48), 5167-5175.

Beaumont, M., Winklehner, S., Veigel, S, Mundigler, N., Gindl-Altmutter, W., Potthast, A., & Rosenau, T. (2020) Wet esterification of never-dried cellulose: a simple process to surface-acetylated cellulose nanofibers. *Green Chemistry*, 22, 5605-5609.

Chen, C., Wang, L., & Huang, Y. (2008). A novel shape-stabilized PCM: electrospun ultrafine fibers based on lauric acid/polyethylene terephthalate composite. *Materials Letters,* 62(20), 3515-3517.

Debenedetti, P. G., & Stillinger, F. H. (2001). Supercooled liquids and the glass transition. *Nature,* 410(6825), 259.

Du, Y., Wu, T., Yan, N., Kortschot, M. T., & Farnood, R. (2014). Fabrication and characterization of fully biodegradable natural fiber-reinforced poly (lactic acid) composites. *Composites Part B: Engineering,* 56, 717-723.

Fashandi, M., & Leung, S. (2017). Preparation and characterization of 100% bio-based polylactic acid/palmitic acid microcapsules for thermal energy storage. *Materials for Renewable and Sustainable Energy*, 6:14.

Fleischer, A. S. (2015). *Thermal energy storage using phase change materials: fundamentals and applications*: Springer.

Gulfam, R., Zhang, P., & Meng, Z. (2019). Advanced thermal systems driven by paraffin-based phase change materials–A review. *Applied energy,* 238, 582-611.

Guo, J., Filpponen, I., Su, P., Laine, J., & Rojas, O. J. (2016). Attachment of gold nanoparticles on cellulose nanofibrils via click reactions and electrostatic interactions. *Cellulose,* 23(5), 3065-3075.

Hassabo, A. G., & Mohamed, A. L. (2017). Enhancement the thermo-regulating property of cellulosic fabric using encapsulated paraffins in modified pectin. *Carbohydrate polymers,* 165, 421-428.

Huo, X., Li, W., Wang, Y., Han, N., Wang, J., Wang, N., & Zhang, X. (2018). Chitosan composite microencapsulated comb-like polymeric phase change material via coacervation microencapsulation. *Carbohydrate polymers,* 200, 602-610.

Kalashnikova, I., Bizot, H., Cathala, B., & Capron, I. (2011). New Pickering emulsions stabilized by bacterial cellulose nanocrystals. *Langmuir,* 27(12), 7471-7479.

Khoo, R., Ismail, H., & Chow, W. (2016). Thermal and morphological properties of poly (lactic acid)/nanocellulose nanocomposites. *Procedia Chemistry,* 19, 788-794.

Kośny, J. (2015). *PCM-enhanced building components: an application of phase change materials in building envelopes and internal structures*: Springer.

Li, J., Lu, W., Zeng, Y., & Luo, Z. (2014). Simultaneous enhancement of latent heat and thermal conductivity of docosane-based phase change material in the presence of spongy graphene. *Solar Energy Materials and Solar Cells,* 128, 48-51.

Li, M., Wu, Z., & Tan, J. (2012). Properties of form-stable paraffin/silicon dioxide/expanded graphite phase change composites prepared by sol–gel method. *Applied energy,* 92, 456-461.

Li, W., Song, G., Tang, G., Chu, X., Ma, S., & Liu, C. (2011). Morphology, structure and thermal stability of microencapsulated phase change material with copolymer shell. *Energy,* 36(2), 785-791.

Li, Y., Yu, S., Chen, P., Rojas, R., Hajian, A., & Berglund, L. (2017). Cellulose nanofibers enable paraffin encapsulation and the formation of stable thermal regulation nanocomposites. *Nano Energy,* 34, 541-548.

Lin, Y., Zhu C., Alva, G., & Fang, G. (2018). Microencapsulation and thermal properties of myristic acid with ethyl cellulose shell for thermal energy storage. *Applied Energy*, 231, 494-501.

Mahfuz, M., Anisur, M., Kibria, M., Saidur, R., & Metselaar, I. (2014). Performance investigation of thermal energy storage system with Phase Change Material (PCM) for solar water heating application. *International Communications in Heat and Mass Transfer,* 57, 132-139.

Maleki, M., Ahmadi, P. T., Mohamdi, H., Karimian, H., Ahmadi, R., & Emrooz, H. B. M. (2019). Photo-thermal conversion structure by infiltration of paraffin in three dimensionally interconnected porous polystyrene-carbon nanotubes (PS-CNT) polyHIPE foam. *Solar Energy Materials and Solar Cells,* 191, 266-274.

Mariano, M., Cercená, R., & Soldi, V. (2016). Thermal characterization of cellulose nanocrystals isolated from sisal fibers using acid hydrolysis. *Industrial Crops and Products,* 94, 454-462.

Meng, Y., Majoinen, J., Zhao, B., & Rojas, O. (2020). Form-stable phase change materials from mesoporous balsa after selective removal of lignin. *Composites Part B*, 199, 108296.

Mikulcová, V., Bordes, R., & Kašpárková, V. (2016). On the preparation and antibacterial activity of emulsions stabilized with nanocellulose particles. *Food Hydrocolloids,* 61, 780-792.

Mondal, S. (2008). Phase change materials for smart textiles–An overview. *Applied thermal engineering,* 28(11-12), 1536-1550.

Nogi, M., Abe, K., Handa, K., Nakatsubo, F., Ifuku, S., & Yano, H. (2006). Property enhancement of optically transparent bionanofiber composites by acetylation. *Applied physics letters,* 89(23), 233123.

Perera, F. (2018). Pollution from fossil-fuel combustion is the leading environmental threat to global pediatric health and equity: Solutions exist. *International journal of environmental research and public health,* 15(1), 16.

Qi, M. (2017). Sunflower Stalk Pith Fibre: Investigation on Oil Holding Capacity, Oil-Fibre Interaction, and Related Application in Food.

Qian, Y., Han, N., Zhang, Z., Cao, R., Tan, L., Li, W., & Zhang, X. (2019). Enhanced Thermal-to-Flexible Phase Change Materials Based on Cellulose/Modified Graphene Composites for Thermal Management of Solar Energy. *ACS applied materials & interfaces,* 11(49), 45832-45843.

Ren, X., Shen, H., Yang, Y., & Yang, J. (2019). Study on the properties of a novel shape-stable epoxy resin sealed expanded graphite/paraffin composite PCM and its application in buildings. *Phase Transitions,* 92(6), 581-594.

Safari, A., Saidur, R., Sulaiman, F., Xu, Y., & Dong, J. (2017). A review on supercooling of Phase Change Materials in thermal energy storage systems. *Renewable and Sustainable Energy Reviews,* 70, 905-919.

Sarier, N., & Onder, E. (2012). Organic phase change materials and their textile applications: an overview. *Thermochimica Acta,* 540, 7-60.

Shchukina, E., Graham, M., Zheng, Z., & Shchukin, D. (2018). Nanoencapsulation of phase change materials for advanced thermal energy storage systems. *Chemical Society reviews,* 47(11), 4156-4175.

Sheng, N., Nomura, T., Zhu, C., Habazaki, H., & Akiyama, T. (2019). Cotton-derived carbon sponge as support for form-stabilized composite phase change materials with enhanced thermal conductivity. *Solar Energy Materials and Solar Cells,* 192, 8-15.

Singh, S., Gaikwad, K. K., Lee, M., & Lee, Y. S. (2018). Microwave-assisted micro-encapsulation of phase change material using zein for smart food packaging applications. *Journal of Thermal Analysis and Calorimetry,* 131(3), 2187-2195.

Svagan, A. J., Musyanovych, A., Kappl, M., Bernhardt, M., Glasser, G., Wohnhaas, C., . . . Landfester, K. (2014). Cellulose nanofiber/nanocrystal reinforced capsules: A fast and facile approach toward assembly of liquid-core capsules with high mechanical stability. *Biomacromolecules,* 15(5), 1852-1859.

Taib, M. N. A. M., Yehye, W. A., Julkapli, N. M., & Hamid, S. B. O. A. (2018). Influence of Hydrophobicity of Acetylated Nanocellulose on the Mechanical Performance of Nitrile Butadiene Rubber (NBR) Composites. *Fibers and Polymers,* 19(2), 383-392.

Tang, Q., Sun, J., Yu, S., & Wang, G. (2014). Improving thermal conductivity and decreasing supercooling of paraffin phase change materials by n-octadecylamine-functionalized multi-walled carbon nanotubes. *RSC Advances,* 4(69), 36584-36590.

Telkes, M. (1980). Thermal energy storage in salt hydrates. *Solar Energy Materials,* 2(4), 381-393.

Tripathi, A., Ago, M., Khan, S. A., & Rojas, O. J. (2018). Heterogeneous Acetylation of Plant Fibers into Micro-and Nanocelluloses for the Synthesis of Highly Stretchable, Tough, and Water-Resistant Co-continuous Filaments via Wet-Spinning. *ACS applied* *materials & interfaces,* 10(51), 44776-44786.

Veerakumar, C., & Sreekumar, A. (2016). Phase change material based cold thermal energy storage: Materials, techniques and applications–A review. *international journal of refrigeration,* 67, 271-289.

Wadsö, L. (1995). CapilIarity in wood and related concepts; a critical review. *Report TVBM,* 3069.

Wei, J., Zhou, Y., Lv, Y., Wang, J., Jia, C., Liu, J., . . . Shao, Z. (2019). Carboxymethyl cellulose nanofibrils with tree-like matrix: preparation and behavior of Pickering emulsions stabilization. *ACS Sustainable Chemistry & Engineering*.

Xiao, X., & Zhang, P. (2013). Morphologies and thermal characterization of paraffin/carbon foam composite phase change material. *Solar Energy Materials and Solar Cells,* 117, 451-461.

Yang, S., Xie, Q., Liu, X., Wu, M., Wang, S., & Song, X. (2018). Acetylation improves thermal stability and transmittance in FOLED substrates based on nanocellulose films. *RSC Advances,* 8(7), 3619-3625.

Yazdani, M., Etula, J., Zimmerman, J., & Seppälä, A. (2020). Ionic cross-linked polyvinyl alcohol tunes vitrification and cold-crystallization of sugar alcohol for long-term thermal energy storage. *Green Chem*., 2020, 22, 5447-5462.

Yoo, Y., Martinez, C., & Youngblood, J. P. (2017). Synthesis and characterization of microencapsulated phase change materials with poly (urea− urethane) shells containing cellulose nanocrystals. *ACS Applied Materials & Interfaces,* 9(37), 31763-31776.

Zhao, Q., Yang, W., Zhang, H., He, F., Yan, H., He, R., Fan, J. (2019). Graphene oxide Pickering phase change material emulsions with high thermal conductivity and photo-thermal performance for thermal energy management. *Colloids and Surfaces A,* 575, 42-49.

Table of Content Graphics

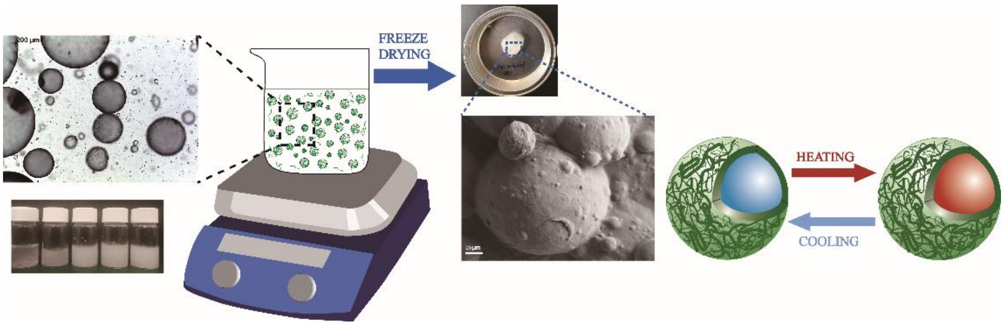

Acetylated cellulose nanofibrils are used to encapsulate paraffin, forming shape-stable phase change systems suitable for thermal energy storage and conversion.